DEVELOPMENT OF A PILOT LOW TEMPERATURE SOLAR THERMAL CO-GENERATION SYSTEM FOR WATER DISTILLATION AND ENERGY GENERATION

Jacobus G. van Zyl[1], Michael T.F. Owen[2], and Gerald Müller[3]

[1] Stellenbosch University – Solar Thermal Energy Research Group (STERG); E-Mail: cobusvanzyl123@gmail.com

[2] Stellenbosch University, 1 Joubert Street, Stellenbosch, 7600, South Africa; Phone: +27-713596654; E-Mail: mikeowen@sun.ac.za

[3] University of Southampton; E-mail: g.muller@soton.ac.uk

Abstract: A solar-thermal system for co-generation of distilled water and energy was investigated in a collaborative study by the University of Southampton and Stellenbosch University. The system utilises a condensing engine, using solar-generated steam at ~1 atm (abs) and a vacuum generated by condensation. The study entailed the design, manufacture, commissioning and testing of a 6.5 kW_{th} prototype system. From on-sun testing, the average daily specific energy consumption (SEC) for water distillate production was 2125 kWh_{GTI}/m^3; and the average daily theoretical solar-to-mechanical energy conversion efficiency was 0.79 %. The SEC was determined to be significantly higher than existing alternatives such as solar PV reverse osmosis, and the energy generation significantly lower compared to commercial solar power technology (e.g. solar PV). As such, the performance and experience gained with the prototype suggest this system is not feasible.

Keywords: co-generation; compound parabolic collector; desalination; solar thermal energy; steam expansion;

Nomenclature

A_{ap}	[m^2]	Aperture area
c_p	[J/kg K]	Specific heat capacity
d_o	[mm]	Outer diameter
ΔT	[K]	Change in temperature
η_{coll}	[%]	Collector solar-to-thermal efficiency
η_0	[%]	Optical efficiency
η_{th}	[%]	Thermal efficiency
GTi	[W/m^2]	Global tilt (in-plane) irradiance
GTI	[kWh/m^2]	Global tilt (in-plane) irradiation
L_{coil}	[m]	Boiler heat-exchanger coil length
$\dot{m}_{st}$	[g/s]	Steam mass flowrate
P_{eo}	[bar (abs)]	Condenser (engine exhaust) pressure
P_s	[bar (abs)]	Cylinder inlet pressure
$\dot{Q}_b$	[W]	Boiler heat gain
$\dot{Q}_u$	[W]	Collector useful heat gain
r_{exp}	–	Expansion ratio
SEC	[kWh/m^3]	Specific energy consumption
T_{in}	[°C]	Outlet temperature
T_{in}	[°C]	Inlet temperature
V_c	[m^3]	Condensate volume collected
V_{clear}	[m^3]	Clearance volume (clearance height x bore area)
V_{exh}	[m^3]	Exhaust volume (exhaust port height x bore area)
$\dot{W}_o$	[W]	Mechanical output power

1 Introduction

In the global transition towards renewable and sustainable energy systems and equitable supply of energy and water resources, Southern Africa is a region of particular interest. This region has large rural populations, who often lack access to energy and clean water, while boasting abundant clean energy resources, including a notable solar resource. In a collaborative effort, Stellenbosch University (SU) and the University of Southampton (UoS) are investigating a low-temperature solar thermal co-generation system for combined water distillation and energy generation. The system couples a compound parabolic solar thermal collector, for steam generation (and thus distillation) at ~1 atm (abs), with a reciprocating steam expander (developed by UoS) to provide a theoretically simple, robust and safe co-generation system. In a parallel study, Reed and Owen [1] simulated the potential performance of the system and concluded that the system was unlikely to be competitive with alternatives such as solar photovoltaic-powered reverse osmosis (PV-RO) and direct PV power generation. Their work included several simplifying assumptions and requires data for validation. Despite the questionable feasibility of the system, the component performance and technical challenges facing the operation of such a system remain interesting. This paper presents the system concept and describes a 6.5 kW_{th} prototype developed at SU. At the time of writing, the steam expander was not yet operational and this paper includes results from the testing of the solar thermal system, and a preliminary (theoretical) analysis of the overall system output and efficiency.

2 System Description

Figure 1 shows the layout of the experimental system. The system consists of two primary sub-systems. The solar steam generation system (SSGS) includes the solar collector array, the boiler and the feed water supply tank. The condensing engine includes the reciprocating steam expander and condenser.

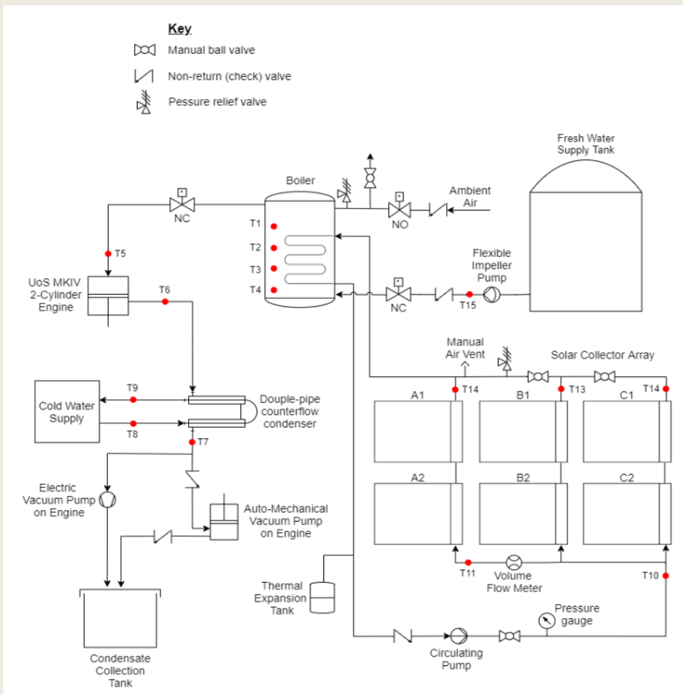

Figure 1 System P&ID

Details of the measurement equipment used in the study are given in Table 1. In addition to the measurement equipment shown in Figure 1, a pyranometer was installed on the collector mounting frame for direct measurement of global tilt irradiance (GTi), condensate volume flow was measured manually at regular intervals to determine the condensate production rate, and pressure transducers were used in the boiler, engine, and condenser.

Table 1 Measurement equipment

Equipment	Measurement	Resolution/ Accuracy
T-type thermocouples x15	Temperature	Error < 1°C. 10-s intervals.
DMP 331 pressure transducers x4	Absolute pressure	Error < 0.35 %. 10-s intervals.
Winsmeter TH7 volume flowmeter x1	HTF volume flowrate	Error < 0.6 %. 10-s intervals.
KIPP and ZONEN CMP6 pyranometer x1	GTi	Error < 5%. 10-s intervals.
Laboratory measuring beakers x3	Volume of condensate	5-mL resolution.

2.1 Solar Steam Generation System (SSGS)

The system uses six external compound parabolic concentrating (XCPC) solar thermal collectors (Figure 2) connected in three parallel rows of two collectors each (see Figure 1). These non-tracking, non-imaging concentrating collectors utilize global (beam + diffuse) tilt solar irradiance to heat the heat transfer fluid (HTF) circulating through the collector array in a closed loop. Liquid water (pressurized to avoid boiling in the collector loop itself) provides a safe, affordable, and readily available HTF.

Figure 2 Solar collector array before pipe insulation

Each XCPC consists of three metal-glass evacuated tubes, with aluminium parabolic reflectors (aperture area $A_{ap} = 2.41\ m^2$, concentration ratio 1.4 [2] and rated optical efficiency 57%). The evacuated tubes enclose a pentagon-shaped fin and U-shaped copper absorber tube, both coated with a selective absorber coating (absorptivity 93-97 %, emissivity 3-7 % [2]). The collector array was mounted on a large frame and fixed at 30° inclination, facing north**.**

The collector efficiency is defined in Equation (1),

$$\eta_{coll} = \frac{\dot{Q}_u}{GTi \cdot A_{ap}} \qquad (1)$$

where $\dot{Q}_u$ is the useful heat gain (sensible) calculated from the measured enthalpy change in the HTF – Equation (2).

$$\dot{Q}_u = \sum_{i=A}^{C} (\dot{m}\, c_p\, \Delta T_{io})_i \tag{2}$$

where *i* represents row A, B or C in Figure 1, $\dot{m}_i$ is the HTF mass flowrate through the two collectors in the respective row, $c_{p,i}$ is the specific heat capacity of liquid water at the bulk mean temperature (mean of row inlet and outlet temperatures), and $\Delta T_{io,i}$ is the temperature rise over the row (e.g. $T_{14} - T_{10}$ for row C in Figure 1).

Steam is generated indirectly in a 70-litre kettle-type boiler (see Figure 3) with a helical coil heating element (L_{coil} = 9 m, d_o = 25 mm) carrying the HTF from the solar collectors. The boiler and collector were sized together to operate in the nucleate boiling regime, with the boiler pressure being approximately 1 atm (abs) and always below 1.5 bar (abs). Indirect steam generation was selected to limit fouling in the solar absorber tubes and facilitate easier maintenance through periodic blowdown and cleaning of the boiler.

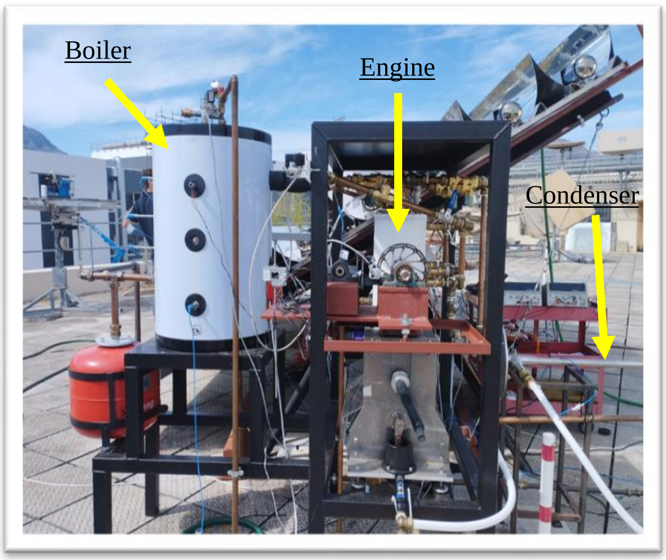

Figure 3 Side view of the system showing the boiler, engine and condenser

The boiler is equipped with various temperature and pressure sensors (the latter controlling the valve between the boiler and the engine); a pressure relief valve (for passive safety); a vacuum breaker; a blowdown port; and connectors for the HTF, feedwater, and steam.

The heat gain by the boiler is equal to the sensible heat loss of the HTF as it passes through the coil, determined using the total HTF enthalpy change through the helical coil – Equation (3).

$$\dot{Q}_b = \dot{m}\, c_p\, (T_{in} - T_{out}) \tag{3}$$

Feedwater is supplied from a 500-litre storage tank by a pump controlled by a float switch in the boiler. The water level in the boiler is kept relatively constant to avoid large influxes of cold water and quenching of the boiler pool.

The SSGS was sized to supply the engine with steam at a rate of 4.36 L/s at 1 bar (abs), equating to 2.56 g/s of saturated vapor The sizing was done using a collector-boiler model constructed in MATLAB, for a clear day with a peak GTi of 900 W/m^2, (which is the overall average daily peak for the test location taken from data for the year 2021 [3]).

2.2 Condensing Engine

A two-cylinder uniflow condensing engine (reciprocating steam expander and condenser) was designed to generate mechanical power from the steam supplied by the SSGS. The steam expander was designed by UoS and manufactured by SU.

2.2.1 Reciprocating steam expander

The piston-cylinder steam expander is shown in Figure 4 (100 mm bore diameter, 160 mm stroke, 3.7 mm clearance height, and 10 mm exhaust port length).

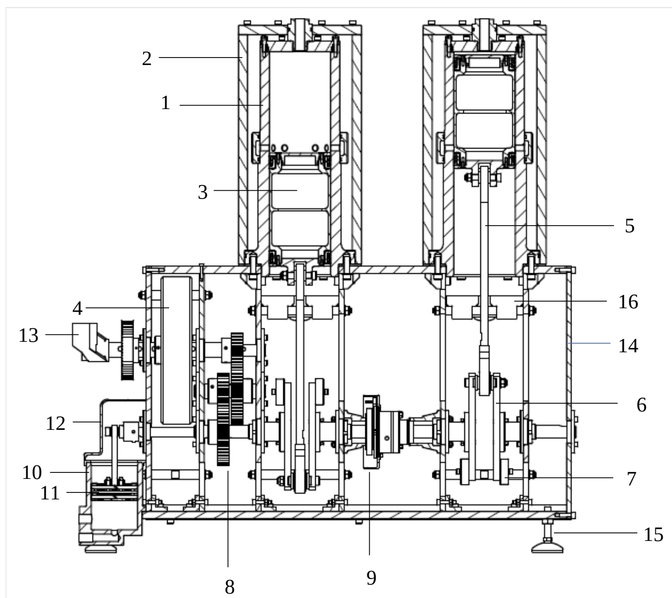

Figure 4 Engine CAD (by UoS) front view, partial section

The major components in Figure 4 are: (1) cylinder, (2) cylinder jacket, (3) piston assembly, (4) flywheel, (5) conrod, (6) crank, (7) counterweight, (8) gear train, (9) position sensor assembly, (10) auto-mechanical vacuum pump (AMVP) cylinder, (11) AMVP piston assembly, (12) AMVP housing, (13) starter handle, (14) aluminium frame and bearing housings, (15) adjustable feet, and (16) drip tray.

2.2.2 Basic Operating Principles

The engine was designed to operate between 60 and 120 rpm. A single revolution of the engine includes one downstroke and one upstroke for both pistons, which equates to a single revolution of the crankshaft and four revolutions of the output shaft. During engine operation, steam is injected alternately into the top of cylinder 1 and 2, prompted by the engine position sensor. Each cylinder has both a supply and exhaust solenoid valve at its inlet, in addition to the exhaust ports in the cylinder which are exposed at the bottom of the downstroke.

The motive force for the engine is the pressure difference across the piston (bottom surface exposed to ambient, top surface exposed alternately to steam / vacuum). The thermodynamic cycle, illustrated in Figure 5, begins with the piston at TDC (5).

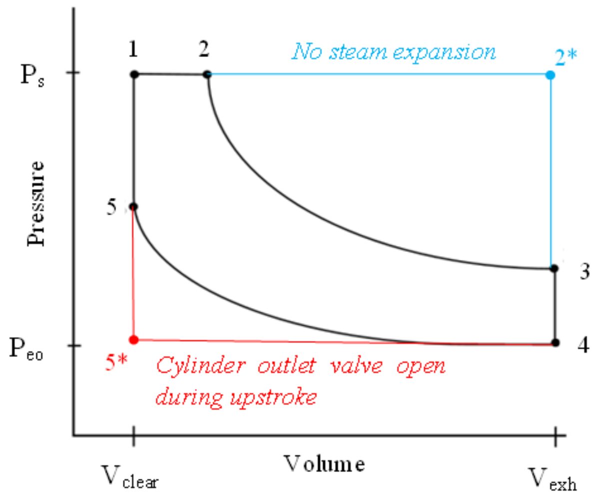

Figure 5 P-V diagram for full condensing engine cycle

The inlet valve opens and steam is supplied, initially at ~1 bar (5-1), before the downstroke begins. The piston is pulled downwards by the momentum of the engine (the pressure on either side of the piston is similar at this stage). The inlet valve remains open for the initial part of the downstroke (1-2, constant pressure). If the valve is closed, then the cycle follows an isothermal expansion process (2-3), with a steam jacket around the cylinder providing the additional heat input. Expansion ratios up to 1:43 are theoretically possible. Alternatively, the inlet valve can remain open for the downstroke, in which case there is no expansion (2-2*, expansion ratio 1:1). Towards the end of the downstroke, the exhaust ports are exposed and the steam is instantaneously evacuated into the condenser (3-4), which operates under vacuum. The pressure inside the cylinder is now sub-atmospheric and the piston is driven upwards by atmospheric pressure acting on the bottom surface of the piston. The exhaust solenoid valve at the top of the cylinder can be closed (4-5) or open (4-5*) during the upstroke.

2.2.3 Condenser

The condenser is critical to the operation of the condensing engine since it maintains the vacuum that results in the net pressure difference across the piston during the upstroke (and thus the motive power). SU's laboratories are equipped with a simple water-cooled, counterflow, double-pipe heat exchanger supplied with cooling water from a water reticulation system (WRS) at ~50 L/min, of sufficient rating. While unlikely to be practical for the eventual system, this condenser provided a convenient solution for the prototype demonstration.

At start-up, an electric vacuum pump is used to evacuate air from the condenser, engine piping and boiler. Once the system is running, the vacuum in the engine is maintained by the AMVP, driven off the engine crankshaft. When the AMVP piston moves upward it creates a vacuum in the AMVP cylinder, drawing the condensate from the condenser. On its downstroke it discharges the condensate into the condensate collection tank.

The volume of collected condensate (V_c) is measured and the Specific Energy Consumption (SEC, kWh/m^3) of the system – Equation (4) – is used to assess and benchmark the water production efficiency of the system.

$$\mathbf{SEC} = \frac{\mathbf{GTI} \cdot \mathbf{A_{ap}}}{\mathbf{V_c}} \tag{4}$$

2.3 Engine Power and Efficiency

The engine performance is measured using the thermal efficiency (η_{th}) defined in Equation (5),

$$\boldsymbol{\eta}_{\mathbf{th}} = \frac{\dot{\mathbf{W}}_{\mathbf{o}}}{\dot{\mathbf{Q}}_{\mathbf{b}}} \tag{5}$$

which is the ratio of mechanical power output to boiler heat gain. The thermal efficiency of the engine was estimated using a linear relationship between the thermal efficiency and engine expansion ratio: r_{exp} = 1 to 4, corresponding to η_{th} = 2 to 5.5 %, derived from measured data obtained by UoS [4]. The mechanical power output was therefore inferred using Equation (5) and the measured heat input, with a variable thermal efficiency determined at each time step using Equation (6).

$$\mathbf{r_{exp}} = \mathbf{max}\left[\mathbf{1}\,;\, \frac{\mathbf{2.56\ g/s}}{\dot{\mathbf{m}}_{\mathbf{st}}}\right] \tag{6}$$

3 Results

Results for three 8-hour SSGS performance tests (14, 16 and 18 February 2023) are reported here. The generated steam was passed through the piping and solenoid valves that connect the SSGS to the engine and the engine to the condenser (to emulate the real pressure losses in the system). Issues with maintaining vacuum have prevented successful operation of the engine to-date. Theoretical engine output is thus estimated based on the expected thermal efficiency and measured SSGS performance. Tests were carried out at SU's Solar Rooftop Laboratory (33.92810°S, 18.86540°E). Test results are extended to theoretically estimate annual yield from the system.

3.1 Solar Input

All three days of testing are considered good solar days during the global-south summer. Figure 6 presents the measured GTi distribution. Cloudy periods on 14-Feb are excluded from this analysis (dashed lines in the figures) as they add no further value to the conclusions drawn.

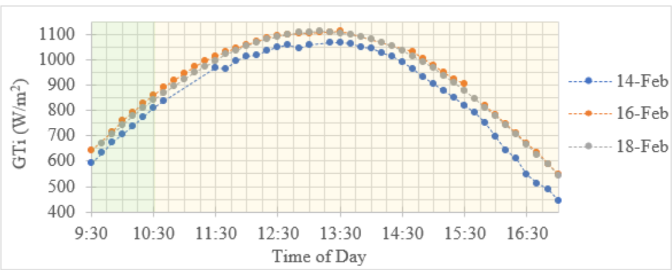

Figure 6 Measured global tilt (in-plane) irradiance

The section highlighted in green in Figure 6 is the ramp-up period during which the boiler water is sensibly heated to its saturation temperature. The in-operation period, when the boiler was generating steam, is indicated in yellow. The peak GTi on 14, 16 and 18 February were 1065, 1110 and 1110 W/m^2, respectively.

3.2 System Output

Figure 7 shows the steam generation rate for the three test periods. Steam was generated at (or above) the required rate of 2.56 g/s during the middle part of the day for all three tests (2-3 hours), reaching a maximum of 2.65, 2.79, and 2.85 g/s; with a mean value of 2.10, 2.10, and 2.25 g/s on 14, 16, and 18 February, respectively. Seeing as the tests were conducted on good solar days, the results suggest the SSGS would require upsizing to meet the required rate during winter and to increase the duration of full-load generation during summer. The inclusion of thermal energy storage (TES) to store the excess thermal energy during peak solar hours may be of benefit. Furthermore, as with any solar powered system, the variable rate of heat input, and associated variations in steam generation (and condition) in this case, would need to be accounted for through careful valve control and / or energy storage to result in steady operation of the engine.

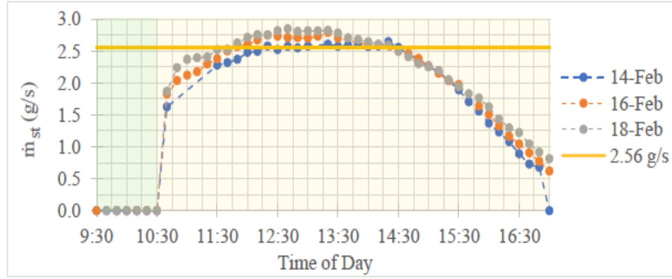

Figure 7 Rate of steam production

The average daily SEC was 2125 kWh$_{GTI}$/m^3, with the hourly distribution shown in Figure 8.

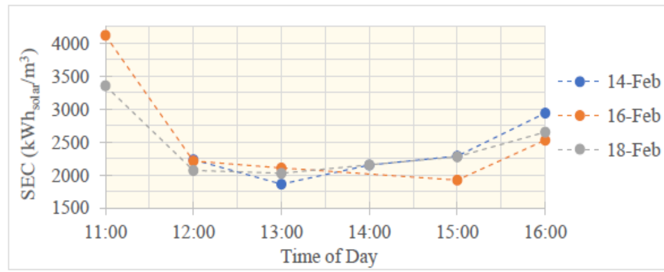

Figure 8 Solar-to-distillate specific energy consumption

Furthermore, the inferred mechanical power output is presented in Figure 9, which gives an average daily solar-to-mechanical energy conversion efficiency of 0.79 %.

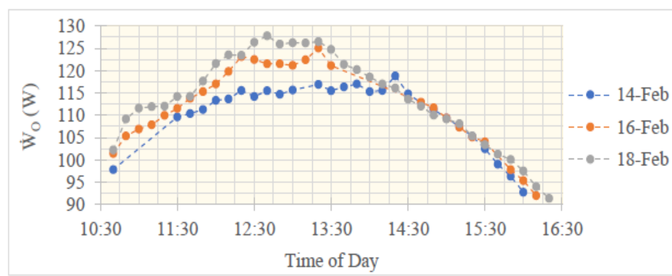

Figure 9 Theoretical mechanical power output

3.3 Annual Performance

Based on the average daily SEC and solar-to-mechanical efficiency, the annual water and power production were estimated using monthly satellite GTI data for the test location from SOLARGIS [5]. The total annual GTI for the test location is 2149.7 kWh$_{GTI}$/m^2. The system is estimated to produce an annual specific mechanical power output of 17.1 kWh/m^2, with the monthly distribution illustrated in Figure 10, which also shows the electrical output assuming a mechanical to electric efficiency of 80 % [6], as well as the monthly distillate production, equating to an annual output of 1012 L/m^2 and average daily output of approximately 2.8 L/m^2.

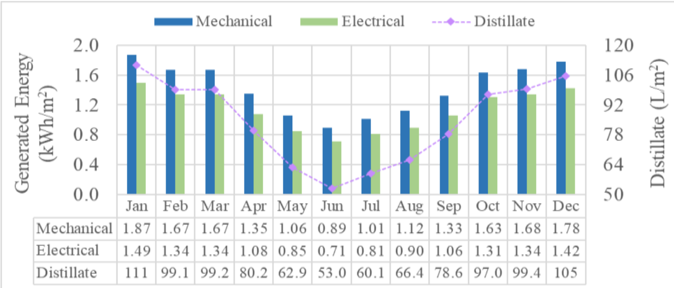

Figure 10 Monthly specific mechanical power and distillate production

To assess the practicality / feasibility of the system investigated in this study, a comparison is made to a solar PV-powered co-generation system consisting of a PV-RO water purification system (SEC as low as 4 kWh_{solar}/m^3 [7, 8]) and generating additional electricity (PV module efficiency 15 % [8]). The systems are sized to generate ~50 kWh_e/month (Free Basic Electricity grant in South Africa [9]) in winter (average of 127.1 kWh_{GTI}/month) at the test location.

The results of the comparison are shown in Table 2 and indicate that the investigated system is not feasible since a PV-powered alternative is significantly more compact to produce the same amount of electricity and cean water, makes use of much less complex and more mature technology, and will cost significantly less based on total size. The total required PV aperture area is 2.75 m^2 compared to 62.7 m^2 in XCPC aperture area for the system investigated in this study.

Table 2 Comparison with solar PV

System ID	Solar PV		This System
Total Collector Area (m^2)	2.62	0.12	62.7
Approx. Number of Collectors/Panels	2-3		26
Average Electrical Energy Output (kWh/month)	50	–	50.6
Clean Water Output (L/month)	–	3900	3900

4 Conclusion

This paper describes a novel solar thermal clean water and energy co-generation system. A 6.5 kW_{th} prototype was developed as part of this work and this paper presents measured results for the steam / distillate production along with theoretical energy generation predictions. At the time of writing, the engine was not operational and getting the full system to operate has proven challenging. The results obtained show the SEC and solar-to-mechanical energy efficiency are notably poor compared to commercially available technologies such as solar PV reverse osmosis and PV power generation, suggesting that this system is not technically feasible. Furthermore, the investigated system is notably more complex and expensive. The condensing engine is nonetheless an intriguing prospect for waste heat recovery (avoiding the need for a dedicated solar thermal steam generation system) and the XCPC collectors have shown good thermal performance and are of interest for industrial process heat applications.

5 References

1. Reed, M., Owen, M. 2023. Simulation of a Novel Combined Water Purification and Electricity Generation System. *17th International Heat Transfer Conference*, Cape Town, 14 – 18 Aug 2023.
2. Artic Solar Inc. 2021. External Concentrating Parabolic Collector (XCPC). Available: https://articsolar.com/wp-content/uploads/2017/08/XCPC-Specifications-102716-Copy-1.pdf
3. Brooks, M., du Clou, S., van Niekerk, J., Gauche, P., Leonard, C., Mouzouris, M., Meyer, A., van der Westhuizen, N., van Dyk, E. & Vorster, F. 2015. SAURAN: A New Source for Solar Radiometric Data in Southern Africa. Journal of Energy in Southern Africa. 26:2–10. Available: https://sauran.ac.za/.
4. Müller, G., Chan, C.H., Gibby, A., Nazir, M.Z., Paterson, J., Seetanah, J., Telfer, M., Tsuzaki, T., Walker, C. & Yusof, F. 2018. The condensing engine: A heat engine for operating temperatures of 100 °C and below. Proceedings of the Institution of Mechanical Engineers, Part A: Journal of Power and Energy. 232(4):437–448. DOI: 10.1177/0957650917736455.
5. SOLARGIS. 2022. Solar Resource Maps and GIS Data for 200+ Countries and Regions. Available: https://solargis.com/maps-and-gis-data/download/world.
6. Müller, G. & Howell, C. 2021. Comparative analysis of ORC and condensing heat engines for low grade waste heat recovery. Applied Engineering. 5(1):29–35. DOI: 10.11648/j.ae.20210501.15.
7. Stillwell, A.S. & Webber, M.E. 2016. Predicting the specific energy consumption of reverse osmosis desalination. Water (Switzerland). 8(12). DOI: 10.3390/w8120601.
8. Rashid, F., Saleem, E.A., Kashif Mehmood, E. & Faizan Rashid, E. 2019. The efficiency of solar PV system. Proceedings of the 2nd International Multi-Disciplinary Conference. Available: https://www.researchgate.net/publication/334277230.
9. Department of Energy. 2012. A survey of energy-related behaviour and perceptions in South Africa. Available: https://www.energy.gov.za/files/media/Pub/Survey%20of%20Energy%20related%20behaviour%20and%20perception%20in%20SA%20-%20Residential%20Sector%20-%202012.pdf.